engineering proceedings

MDPI

Proceeding Paper

Structural Health Monitoring Strategy Based on Adaptive Kalman Filtering

Haodong Qiu *, Luca Rosafalco, Aldo Ghisi and Stefano Mariani

Department of Civil and Environmental Engineering, Politecnico di Milano, Piazza L. da Vinci 32, 20133 Milano, Italy; luca.rosafalco@polimi.it (L.R.); aldo.ghisi@polimi.it (A.G.); stefano.mariani@polimi.it (S.M.)
* Correspondence: haodong.qiu@polimi.it

Abstract: Structures are exposed to aging and extreme events that can decrease the relevant safety margins or even lead to (partial) collapse mechanisms under unforeseen loading conditions. Structural health monitoring (SHM) looks therefore compulsory to avoid accidents, by tracking the evolution of the state of the system and sending out warnings as soon as critical conditions are met or drifts from the response of the undamaged structure are identified. One of the approaches to online SHM rests on Kalman filtering, which is able to build the time evolution of the structural state upon the Bayes' rule. In a customary joint version of the filtering procedure, state variables and health parameters are joined together in an extended state vector: while state variables, like e.g., lateral displacements of shear buildings, can be observed thanks to pervasive sensor networks, the health parameters usually linked to the structural stiffness cannot, leading to possible divergence issues characterized by biases in the estimates. These issues are further enhanced by difficulties in setting the covariance terms, whose initialization is required to utilize Kalman filters. In this work, we investigate an adaptive strategy to the online tuning of the aforementioned covariance terms, leading to an improvement of the filter outcomes without issues related to its instability. This procedure is then applied to the SHM of a shear building, to highlight the excellent results in terms of accuracy and robustness.

Keywords: structural health monitoring; extended Kalman filter; adaptive Kalman filtering; damage detection

Citation: Qiu, H.; Rosafalco, L.; Ghisi, A.; Mariani, S. Structural Health Monitoring Strategy Based on Adaptive Kalman Filterin. *Eng. Proc.* **2024**, *1*, 0. https://doi.org/

Academic Editor: Firstname Lastname

Published: 26 November 2024

1. Introduction

Structural health monitoring (SHM) plays a vital role in ensuring the safety, reliability, and longevity of large-scale structures such as bridges, buildings, dams, and wind turbines. It involves the continuous monitoring and assessment of the structural integrity to detect potential defects, damages, or anomalies. Traditional SHM approaches rely on periodic inspections, which may not provide real-time insights into structural health and may lead to delayed detection of critical issues. The global structural health monitoring market size was valued at USD 2210 million in 2021 and is projected to reach USD 7595 million by 2030, growing at a compound annual growth rate of 14.7% during the forecast period [1].

The Extended Kalman Filter (EKF) can simultaneously estimate both structural properties, such as the interstorey stiffness in a shear building, and state by extending the state vector [2,3]. However, the EKF assumes complete knowledge of the process noise covariance and measurement noise covariance matrices, which is difficult to foresee in most cases and this significantly affects the accuracy of estimations. To estimate the process and measurement noise covariances, approaches based on adaptive filtering have been proposed, e.g., by Mehra [4].

In this paper, an adaptive strategy is adopted in conjunction with the EKF on a two-story shear building, aiming to automatically tune the process noise covariance and improve the accuracy and stability of the estimation of the structural stiffness and, therefore, health. The general conclusion is that the Adaptive Extended Kalman Filter (AEKF) not only outperforms the traditional EKF in accuracy, but also demonstrates robustness in multi-parameter estimation and damage detection.

The remainder of the contribution is arranged as follows. Section 2 discusses the structural model and the adaptive Kalman filtering theory here applied. In Section 3, numerical outcomes and estimations by the Kalman filtering procedure are presented, to validate the advantages of the AEKF. In Section 4, some final conclusions are drawn along with proposed further enhancements to deal with realistic structural systems.

2. Materials and Methods

2.1. Structural Model and Data Generation

The considered structure is the two-story shear building shown in Figure 1. Measurement of the lateral displacements of the first and second stories are collected every 0.01 s and are adopted as observations for the Kalman filter. Exploiting the recorded earthquake input employed in [5], the structure is subjected to the relevant equivalent forces over a duration of 40.96 s. An explicit Newmark time integration scheme [6] is employed to generate the pseudo-experimental evolution of the state of the structure via a MATLAB code. The interstorey stiffnesses k_1 and k_2 have to be identified or tuned during the analysis, and may even change in time due to some damage accumulation processes which are indeed not explicitly modeled due to a time scale separation principle, see [7,8].

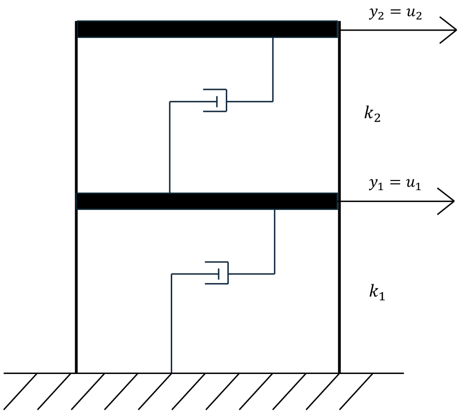

Figure 1. Sketch of the two-story shear building, with lateral displacements of the two stories highlighted.

2.2. Extended Kalman Filter

The EKF, see [9–17], operates on the structural system through the state transition equation:

$$\mathbf{x}_k = \mathbf{f}(\mathbf{x}_{k-1}) + \mathbf{w}_k, \tag{1}$$

and the measurement equation:

$$\mathbf{z}_k = \mathbf{H}\mathbf{x}_k + \mathbf{v}_k, \tag{2}$$

where:

- $\mathbf{x}_k$ is the state vector at time t_k, including in our analysis displacements, velocities, accelerations, and interstorey stiffness values.
- $\mathbf{z}_k$ is the measurement vector at time t_k, consisting of the lateral displacements of the two stories.
- $\mathbf{f}(\cdot)$ is the state transition function, linked to the adopted Newmark time integration procedure. It must be noted that the response of the system is linear, but the operator $\mathbf{f}$ becomes nonlinear due to the inclusion of the stiffness terms in the state vector. Details can be found in Appendix A.
- $\mathbf{H}$ is the observation matrix, describing the relationship between measurements and the state. In this case, it is a Boolean matrix with non-zero entries to select the observed displacements out of the state vector.

- $\mathbf{w}_k$ is the process noise, a zero-mean Gaussian process with covariance $\mathbf{Q}_k$.
- $\mathbf{v}_k$ is the measurement noise, a zero-mean Gaussian process with covariance $\mathbf{R}_k$.

The EKF can be decomposed into 3 main steps:

1. **Initialization**
   It sets the initial guess for the state $\hat{\mathbf{x}}_{0|0}$ and error covariance $\mathbf{P}_{0|0}$.
2. **Prediction**
   The estimate of the predicted state is moved forward in time according to:

$$\hat{\mathbf{x}}_{k|k-1} = \mathbf{f}(\hat{\mathbf{x}}_{k-1|k-1}); \tag{3}$$

   and, if the state transition Jacobian is:

$$\mathbf{F}_{k-1} = \left.\frac{\partial \mathbf{f}}{\partial \mathbf{x}}\right|_{\hat{\mathbf{x}}_{k-1|k-1}}. \tag{4}$$

   then the predicted error covariance reads:

$$\mathbf{P}_{k|k-1} = \mathbf{F}_{k-1}\mathbf{P}_{k-1|k-1}\mathbf{F}_{k-1}^{\top} + \mathbf{Q}_{k-1}. \tag{5}$$

   with $\cdot^{\top}$ standing for transpose.

3. **Update**
   By exploiting the innovation or measurement residuals, defined as the difference between measurements and prediction from the last step according to:

$$\mathbf{y}_k = \mathbf{z}_k - \mathbf{H}\hat{\mathbf{x}}_{k|k-1}; \tag{6}$$

   The innovation covariance can be obtained as:

$$\mathbf{S}_k = \mathbf{H}\mathbf{P}_{k|k-1}\mathbf{H}^{\top} + \mathbf{R}_k, \tag{7}$$

   and the Kalman gain reads:

$$\mathbf{K}_k = \mathbf{P}_{k|k-1}\mathbf{H}^{\top}\mathbf{S}_k^{-1}. \tag{8}$$

   The updated state estimate is retrieved as:

$$\hat{\mathbf{x}}_{k|k} = \hat{\mathbf{x}}_{k|k-1} + \mathbf{K}_k\mathbf{y}_k, \tag{9}$$

   and the updated error covariance is:

$$\mathbf{P}_{k|k} = (\mathbf{I} - \mathbf{K}_k\mathbf{H})\mathbf{P}_{k|k-1}. \tag{10}$$

2.3. Adaptive Extended Kalman Filter

In Kalman filtering, it is usually assumed that the process noise covariance and the measurement noise covariance are known in advance, or can be tuned beforehand on the basis of a trial-and-error procedure. They thus represent a kind of hyperparameters of the numerical procedure. This can be true for $\mathbf{R}_k$, as it is related to the noise level of the measurements and so can be determined from the technical features of the measurement equipment, but it is certainly not for $\mathbf{Q}_k$. An improper selection of $\mathbf{Q}_k$ can lead to significant errors in state estimation, so an adaptive strategy for estimating $\mathbf{Q}_k$ and $\mathbf{R}$ based on the innovation sequence is reported here, see also [18].

Specifically, the process noise covariance can be recursively updated by way of the expected value of the innovation, according to:

$$\mathbf{Q}_{k-1} = \mathbf{K}_k\,\mathbb{E}\left[\mathbf{y}_k\mathbf{y}_k^{\top}\right]\mathbf{K}_{\mathbf{k}}^{\mathbf{T}} \tag{11}$$

where $\mathbb{E}\left[\mathbf{y}_k\mathbf{y}_k^\top\right]$ is usually computed by averaging all the innovation terms at each step of filtering. A so-called forgetting factor α, see also [19], is used to weight the innovation [18,20], so that the estimation of $\mathbf{Q}_k$ over time is:

$$\mathbf{Q}_k = \alpha\,\mathbf{Q}_{k-1} + (1-\alpha)\left(\mathbf{K}_k\mathbf{y}_k\mathbf{y}_k^\top\mathbf{K}_k^\top\right) \tag{12}$$

The value of α obviosuly affects the rate of estimation change. In this work, after a preliminary parametric investigation, α has been set to 0.6, to attain a robust and reliable performance.

3. Results

In this study, the AEKF is compared with the traditional EKF, in terms of accuracy of estimations of the interstorey stiffness(es) of the shear building of Figure 1. In the analysis, the process noise covariance matrix is randomly initialized, to possibly avoid any bias induced by the initial expert guess. First, a single parameter is tuned by assuming that the interstorey stiffness is constant for the building. Next, to investigate the capability of AEKF to handle a multi-parameter estimation problem, a different value of the stiffness is adopted for each interstorey. Finally, to also assess the capability of AEKF to promptly react to changes in the structural health, departing from the second case a reduction of one stiffness is introduced in the analysis, so that the estimation becomes a truly time-dependent problem solution.

In the absence of an accurate know-how in terms of health parameters, the AEKF is shown to be able to automatically adjust the stiffness terms based on the innovation sequence, yielding high-accuracy estimations of both states and structural health. To demonstrate the effectiveness of the AEKF, the results obtained in the three scenarios described above are presented in the following.

3.1. Scenario 1: Single Stiffness Parameter

In this case, the two interstorey stiffness values k_1 and k_2 are assumed to be the same, namely $k_1 = k_2 = 1.4\ \times 10^9$ N/m. To provide a fair comparison, the filters are initialized with the same state estimate and error covariance matrix, as well as the same process and measurement noise covariance matrices, adopting:

$$\hat{\mathbf{x}}_{0|0} = \begin{bmatrix} 0 & 0 & 0 & 0 & 0 & 0 & 1\times 10^9 \end{bmatrix}^\top$$
$$\mathbf{P}_{0|0} = \mathrm{diag}(\underbrace{1\times10^{-10},\ldots,1\times10^{-10}}_{6\text{ times}},1\times10^{14})$$
$$\mathbf{Q}_0 = \mathrm{diag}(\underbrace{1\times10^{-4},\ldots,1\times10^{-4}}_{6\text{ times}},1\times10^{12})$$
$$\mathbf{R}_0 = \mathrm{diag}(8.6\times10^{-9},2.2\times10^{-8},6.3\times10^{-6},1.6\times10^{-5},5.3\times10^{-3},1.4\times10^{-2},1\times10^{16})$$

The AEKF shows a superior performance in relation to the estimates of all the structural state components (displacements $\mathbf{u}$, velocities $\dot{\mathbf{u}}$, and accelerations $\ddot{\mathbf{u}}$). As exemplary results, the time histories of the acceleration estimates for the first story are compared in Figure 2, to illustrate the difference between the filters outcomes. When provided with an inaccurate initial process noise covariance matrix, it is reported that the error in $\ddot{u}_1$ given by the EKF does not decrease in 40.96 s. In contrast, the AEKF provides an error in $\ddot{u}_1$ that diminishes to nearly zero within 10 s, with the estimation remaining consistently convergent with the true value thereafter.

Regarding the estimation of the stiffness, as shown in Figure 3 the traditional EKF performs poorly compared to the AEKF, when an inappropriate process noise covariance is provided. In the EKF, the estimation of the stiffness shows negligible changes and maintains a significant bias away from the true value. In contrast, the AEKF leads to an estimation of stiffness that converges to the true value within 10 s, and further reduces the error over the remaining time.

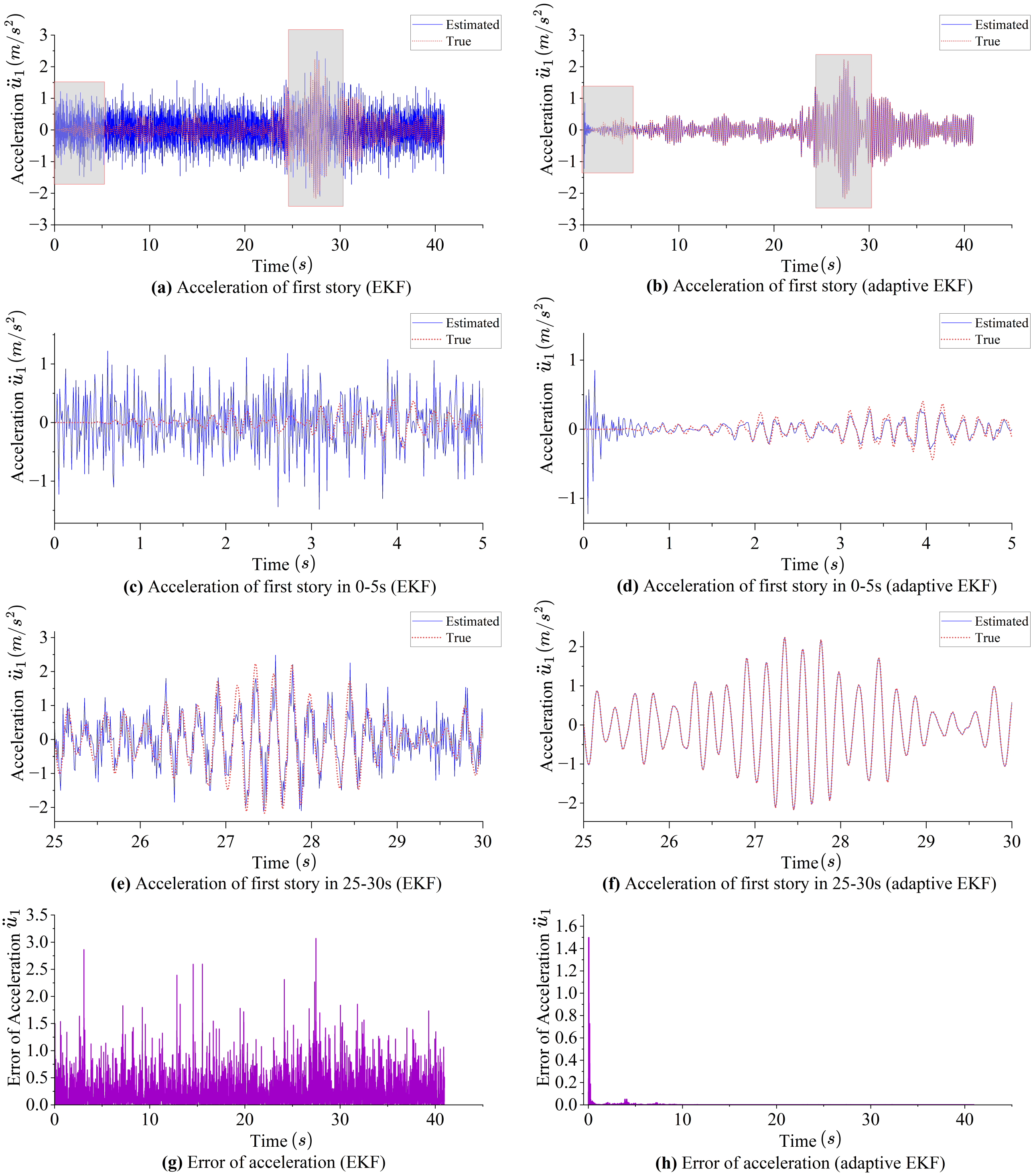

(a) Acceleration of first story (EKF) **(b)** Acceleration of first story (adaptive EKF)
(c) Acceleration of first story in 0-5s (EKF) **(d)** Acceleration of first story in 0-5s (adaptive EKF)
(e) Acceleration of first story in 25-30s (EKF) **(f)** Acceleration of first story in 25-30s (adaptive EKF)
(g) Error of acceleration (EKF) **(h)** Error of acceleration (adaptive EKF)

Figure 2. Scenario 1. Comparison of estimations provided by (**left**) EKF and (**right**) AEKF.

The initial process noise covariance $\mathbf{Q}_0$ is set as diagonal, with entries respectively referring to the story displacements, velocities, and acceleration, and to the interstorey stiffness. The matrix $\mathbf{Q}_{\text{final}}$ reads:

$$\mathbf{Q}_{\text{final}} = \begin{bmatrix} 9\times10^{-12} & 1\times10^{-11} & -3\times10^{-11} & -4\times10^{-11} & -8\times10^{-9} & -1\times10^{-8} & -2 \\ 1\times10^{-11} & 2\times10^{-11} & -4\times10^{-11} & -7\times10^{-11} & -1\times10^{-8} & -2\times10^{-8} & -3 \\ -3\times10^{-11} & -4\times10^{-11} & 3\times10^{-10} & 4\times10^{-10} & 2\times10^{-8} & 4\times10^{-8} & 5 \\ -4\times10^{-11} & -7\times10^{-11} & 4\times10^{-10} & 7\times10^{-10} & 4\times10^{-8} & 7\times10^{-8} & 9 \\ -8\times10^{-9} & -1\times10^{-8} & 2\times10^{-8} & 4\times10^{-8} & 7\times10^{-6} & 1\times10^{-5} & 2\times10^{3} \\ -1\times10^{-8} & -2\times10^{-8} & 4\times10^{-8} & 7\times10^{-8} & 1\times10^{-5} & 2\times10^{-5} & 2\times10^{3} \\ -2 & -3 & 5 & 9 & 2\times10^{3} & 2\times10^{3} & 3\times10^{11} \end{bmatrix}_{7\times7},$$

which is no longer diagonal, and the values of the off-diagonal elements do not result to be negligible compared to the diagonal ones. Further research on more complex structures is required to understand the influence of a non-diagonal $\mathbf{Q}_k$ matrix on the filter outcomes.

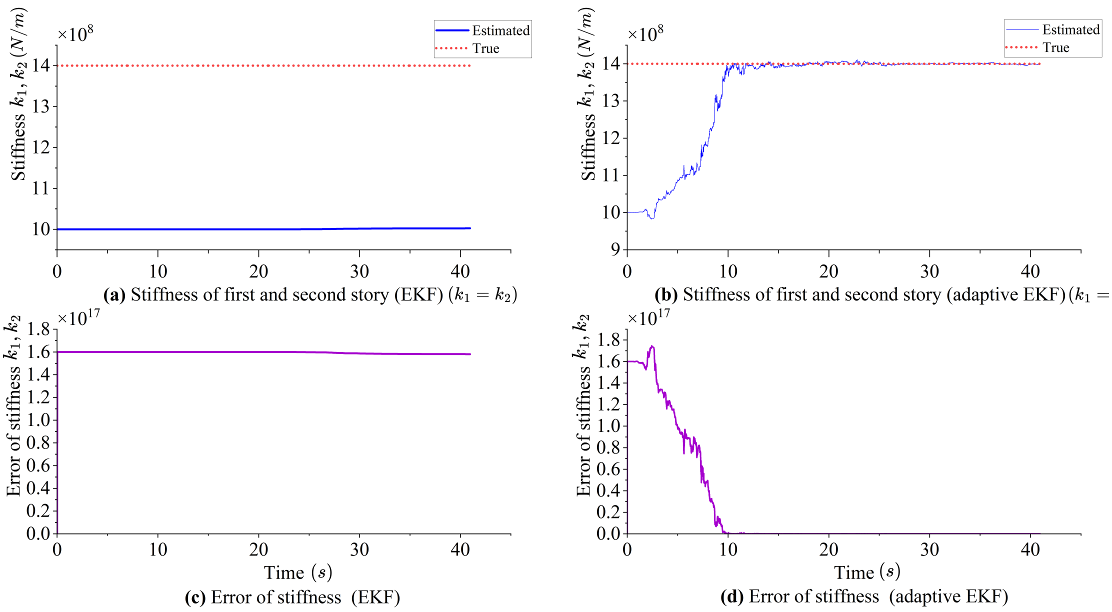

Figure 3. Scenario 1. Comparison of stiffness estimations and relevant errors, as provided by (**left**) EKF and (**right**) AEKF.

Figure 4 shows the time evolution of Q_{77} (in log form) during tuning, to report that it fluctuates around a magnitude of 10^{11} $(\mathrm{N/m})^2$. Despite the true stiffness being 1.4×10^9 N/m, and the expectation that the process noise covariance of stiffness would have a high magnitude, it remains challenging to tune Q_{77} to a higher degree of accuracy.

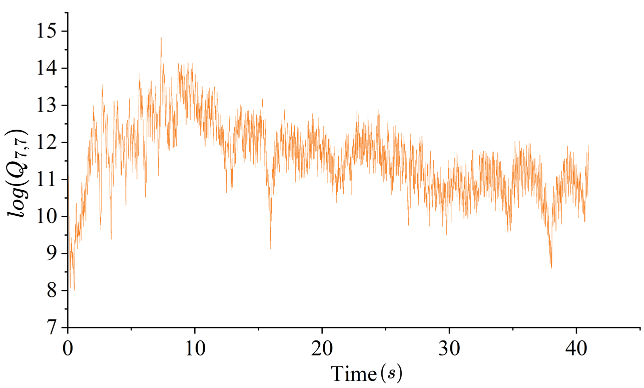

Figure 4. Scenario 1. Time evolution of the process noise covariance term Q_{77} related to the structural stiffness.

3.2. Scenario 2: Multiple Stiffness Estimation

In this case, the shear building is assumed to feature different interstorey stiffness values, so that: $k_1 = 1.4 \times 10^9$ N/m and $k_2 = 1 \times 10^9$ N/m. The initial guesses of stiffness are chosen to be significantly different from the true values: $k_{1,0} = 1 \times 10^9$ N/m and $k_{2,0} = 1.6 \times 10^9$ N/m. As shown in Figure 5, although it takes about 30 s for k_1 and k_2 to converge to the true values, the final estimations exhibit high accuracy and stability. This demonstrates that the AEKF can effectively update the structural model even when multiple structural parameters are unknown.

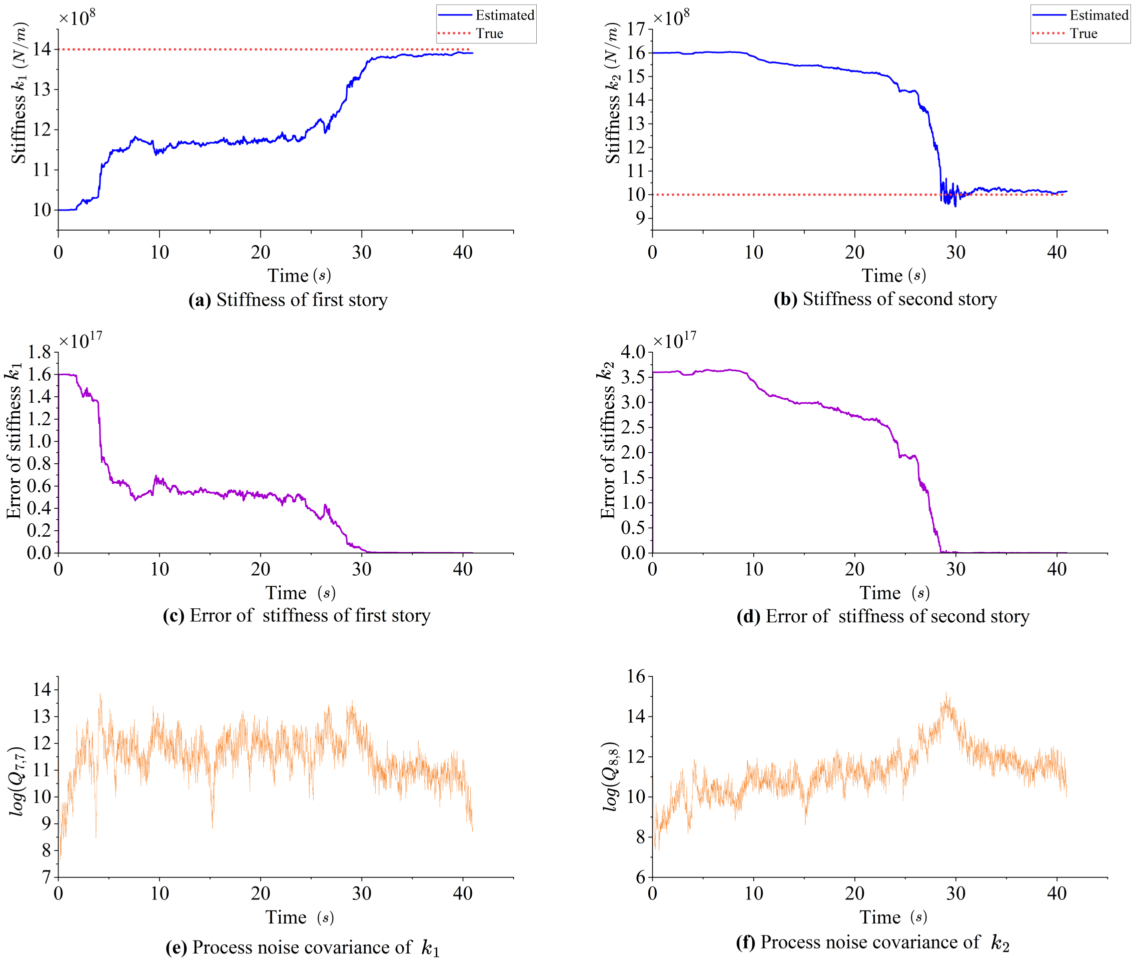

Figure 5. Scenario 2, AEKF results. Estimation of the stiffness terms k_1 and k_2, relevant error evolution, and process noise covariance terms tuning.

3.3. Scenario 3: Multiple Stiffness Estimation in the presence of a Damage Event

To testify that the AEKF can operate under more complex conditions and detect damage, the stiffness k_1 of Scenario 2 is reduced to half at 20 s, so that a damage occurring on the first interstorey in allowed for. As shown in Figure 6, the stiffness estimation reacts quickly to the sudden change of k_1, and it takes approximately 10 s for the estimations of both k_1 and k_2 to converge again to the correct values.

These further results indicate that, as an online SHM method, the adtaptive EKF can detect structural changes and respond promptly by updating the structural parameters. Results of the same quality, even if not shown here for brevity, cannot be obtained with the EKF.

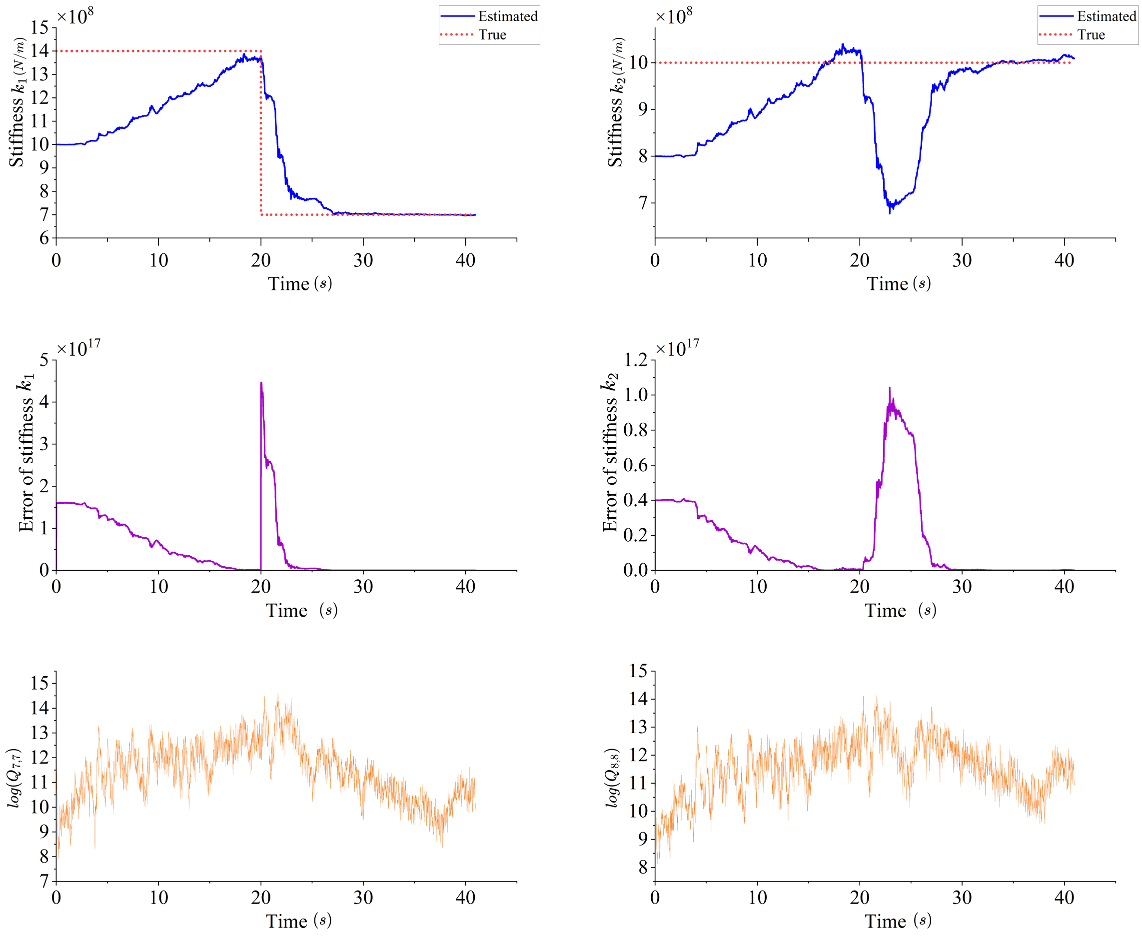

Figure 6. Scenario 3, AEKF results. Estimation of the stiffness terms k_1 and k_2, relevant error evolution, and process noise covariance terms tuning in the presence of a damage on the first interstorey occurring at $t = 20$ s.

4. Discussion

The adaptive extended Kalman filter has been proposed to avoid issues related to the setting of the process noise covariance matrix. By automatically tuning all its entries thanks to the innovation sequence, a significantly improvement of the accuracy of state and stiffness estimations has been achieved. The filter has also demonstrated a good performance in multi-parameter estimation, allowing for the updating of structural parameters related to the stiffness, possibly mimicking the presence of damage even in the absence of direct measurements.

Future research will focus on developing methods to improve the stability and accuracy of the estimation of the process noise covariance. Moreover, a procedure to set the most efficient forgetting factor α will be proposed with the aid of machine learning algorithms. Ultimately, this online SHM method will be enhanced using high-performance computing, to achieve real-time SHM on high-dimensional structures.

Author Contributions: Conceptualization, S.M. and A.G.; methodology, H.Q.; software, H.Q.; validation, A.G., S.M. and L.R.; formal analysis, H.Q.; investigation, H.Q. and L.R.; resources, S.M. and A.G.; data curation, H.Q. and L.R.; writing—original draft preparation, H.Q.; writing—review and editing, L.R., A.G. and S.M.; visualization, H.Q.; supervision, A.G. and S.M. All authors have read and agreed to the published version of the manuscript.

Funding: This work has been partially supported by the Spoke 1 "FutureHPC & BigData" of the ICSC–Centro Nazionale di Ricerca in High Performance Computing, Big Data and Quantum Computing- and hosting entity, funded by European Union–Next GenerationEU.

Institutional Review Board Statement: Not applicable.

Informed Consent Statement: Not applicable.

Data Availability Statement: Data can be obtained by kindly writing to the corresponding author.

Conflicts of Interest: The authors declare no conflicts of interest.

Abbreviations

The following abbreviations are used in this manuscript.

AEKF	Adaptive Extended Kalman Filter
EKF	Extended Kalman Filter
SHM	Structural Health Monitoring

Appendix A

The dynamics of the structural system shown in Figure 1 is governed by the following equation [21]:

$$\mathbf{M}\ddot{\mathbf{u}} + \mathbf{D}(t)\dot{\mathbf{u}} + \mathbf{K}(t)\mathbf{u} = \mathbf{F}(t), \tag{A1}$$

where: t is time; $\mathbf{M}$, $\mathbf{D}$, $\mathbf{K}$ are the mass, damping and stiffness matrices, respectively; $\mathbf{u}$, $\dot{\mathbf{u}}$, $\ddot{\mathbf{u}}$ are the displacement, velocity and acceleration vectors, respectively; $\mathbf{F}$ is the external load vector.

Within each time interval $[t_{n-1} \quad t_n]$, the time marching procedure can be split on its own, into a prediction stage:

$$\begin{aligned} \widetilde{\mathbf{u}}_k &= \mathbf{u}_{k-1} + \Delta t\, \dot{\mathbf{u}}_{k-1} + \Delta t^2 \left(\frac{1}{2} - \beta \right) \ddot{\mathbf{u}}_{k-1} \\ \widetilde{\dot{\mathbf{u}}}_k &= \dot{\mathbf{u}}_{k-1} + \Delta t (1-\gamma) \ddot{\mathbf{u}}_{k-1}, \end{aligned} \tag{A2}$$

an (explicit) integration stage:

$$\ddot{\mathbf{u}}_k = \mathbf{M}^{-1}(\mathbf{F}_k - \mathbf{D}_{k-1}\widetilde{\dot{\mathbf{u}}}_k - \mathbf{K}_{k-1}\widetilde{\mathbf{u}}_k). \tag{A3}$$

and a final correction stage:

$$\begin{aligned} \mathbf{u}_k &= \widetilde{\mathbf{u}}_k + \Delta t^2 \beta \ddot{\mathbf{u}}_k \\ \dot{\mathbf{u}}_k &= \widetilde{\dot{\mathbf{u}}}_k + \Delta t \gamma \ddot{\mathbf{u}}_k, \end{aligned} \tag{A4}$$

where: $\Delta t = t_n - t_{n-1}$ is the time step size (constrained due to algorithmic stability); β and γ are algorithmic parameters, see [22].

The nonlinear function $\mathbf{f}$ in Equation (3) for the structural state can be derived from the equations above, to obtain:

$$\boldsymbol{z}_k = \boldsymbol{A}_k \boldsymbol{z}_{k-1} + \boldsymbol{b}_k \tag{A5}$$

where:

$$\mathbf{A}_k = \begin{bmatrix} \mathbf{I} - \beta\Delta t^2\mathbf{M}^{-1}\mathbf{K}_{k-1} & \Delta t\mathbf{I} - \beta\Delta t^2\mathbf{M}^{-1}(\mathbf{D}_{k-1} + \Delta t\mathbf{K}_{k-1}) & -\beta\Delta t^2\mathbf{M}^{-1}\left(\Delta t^2(1/2 - \beta)\mathbf{K}_{k-1} + \Delta t(1 - \gamma)\mathbf{D}_{k-1}\right) + \Delta t^2(1/2 \\ -\gamma\Delta t\mathbf{M}^{-1}\mathbf{K}_{k-1} & \mathbf{I} - \gamma\Delta t\mathbf{M}^{-1}(\mathbf{D}_{k-1} + \Delta t\mathbf{K}_{k-1}) & -\gamma\Delta t\mathbf{M}^{-1}\left(\Delta t^2(1/2 - \beta)\mathbf{K}_{k-1} + \Delta t(1 - \gamma)\mathbf{D}_{k-1}\right) + \Delta t(1-\gamma)\mathbf{I} \\ -\mathbf{M}^{-1}\mathbf{K}_{k-1} & -\mathbf{M}^{-1}(\mathbf{D}_{k-1} + \Delta t\mathbf{K}_{k-1}) & -\mathbf{M}^{-1}\left(\Delta t^2(1/2-\beta)\mathbf{K}_{k-1} + \Delta t(1-\gamma)\mathbf{D}_{k-1}\right) \end{bmatrix} \tag{A6}$$

$$\mathbf{b}_k = \begin{bmatrix} \beta\Delta t^2\mathbf{M}^{-1}\mathbf{F}_k \\ \gamma\Delta t\mathbf{M}^{-1}\mathbf{F}_k \\ \mathbf{M}^{-1}\mathbf{F}_k \end{bmatrix}$$

being **I** the unit matrix.

As far as the function of stiffness is concerned, a random walk is simply assumed to provide:

$$z_{k,\text{stiffness}} = z_{k-1,\text{stiffness}}. \tag{A7}$$

References

1. Straits Research: Structural Health Monitoring Market Size Is Projected to reach USD 7.59 Billion by 2030, 2022. Available online: https://www.globenewswire.com/en/news-release/2022/08/02/2490603/0/en/Structural-Health-Monitoring-Market-Size-is-projected-to-reach-USD-7-59-Billion-by-2030-growing-at-a-CAGR-of-14-7-Straits-Research.html (accessed on 20 August 2024).
2. Kalman, R.E. A new approach to linear filtering and prediction problems. *J. Basic Eng.* **1960**, *82*, 35–45.
3. Schmidt, S.F. Application of State-Space Methods to Navigation Problems. *Adv. Control. Syst.* **1966**, *3*, 293–340. https://doi.org/10.1016/B978-1-4831-6716-9.50011-4.
4. Mehra, R. Approaches to adaptive filtering. *IEEE Trans. Autom. Control* **1972**, *17*, 693–698. https://doi.org/10.1109/TAC.1972.1100100.
5. Rosafalco, L.; Azam, S.E.; Mariani, S.; Corigliano, A. System Identification via Unscented Kalman Filtering and Model Class Selection. *ASCE-ASME J. Risk Uncertain. Eng. Syst. Part A Civ. Eng.* **2024**, *10*, 04023063. https://doi.org/10.1061/AJRUA6.RUENG-1085.
6. Bathe, K.J., Finite Element Method. In *Wiley Encyclopedia of Computer Science and Engineering*; John Wiley & Sons, Ltd.: Hoboken, NJ, USA, 2008; pp. 1–12. https://doi.org/10.1002/9780470050118.ecse159. Available online: http://arxiv.org/abs/https://onlinelibrary.wiley.com/doi/pdf/10.1002/9780470050118.ecse159 (accessed on).
7. Torzoni, M.; Manzoni, A.; Mariani, S. Structural health monitoring of civil structures: A diagnostic framework powered by deep metric learning. *Comput. Struct.* **2022**, *271*, 106858.
8. Rosafalco, L.; Torzoni, M.; Manzoni, A.; Mariani, S.; Corigliano, A. Online structural health monitoring by model order reduction and deep learning algorithms. *Comput. Struct.* **2021**, *255*, 106604.
9. Kalman, R.E.; Bucy, R.S. New results in linear filtering and prediction theory. *ASME J.* **1961**, *83*, 95–108.
10. Ljung, L. *The Extended Kalman Filter as a Parameter Estimator for Linear Systems*; Linköping University: Linköping, Sweden, 1977.
11. Ljung, L. System identification. In *Signal Analysis and Prediction*; Springer: Berlin/Heidelberg, Germany, 1998; pp. 163–173.
12. Nelson, A.T. *Nonlinear Estimation and Modeling of Noisy Time Series by Dual Kalman Filtering Methods*; Oregon Graduate Institute of Science and Technology: Hillsboro, OR, USA, 2000.
13. Bittanti, S.; Maier, A.N.G. Inverse problems in structural plasticity: A Kalman filter approach. In *Plasticity Today: Modelling, Methods and Applications*; 1984.
14. Bolzon, G.; Fedele, R.; Maier, G. Parameter identification of a cohesive crack model by Kalman filter. *Comput. Methods Appl. Mech. Eng.* **2002**, *191*, 2847–2871.
15. Catlin, D.E. *Estimation, Control, and the Discrete Kalman Filter*; Springer Science & Business Media: Berlin/Heidelberg, Germany, 2012; Volume 71.
16. Wan, E.A.; Nelson, A.T. Dual extended Kalman filter methods. In *Kalman Filtering and Neural Networks*; 2001; pp. 123–173.
17. Hoshiya, M.; Saito, E. Structural identification by extended Kalman filter. *J. Eng. Mech.* **1984**, *110*, 1757–1770.
18. Song, M.; Astroza, R.; Ebrahimian, H.; Moaveni, B.; Papadimitriou, C. Adaptive Kalman filters for nonlinear finite element model updating. *Mech. Syst. Signal Process.* **2020**, *143*, 106837. https://doi.org/10.1016/j.ymssp.2020.106837.
19. Mariani, S.; Corigliano, A. Impact induced composite delamination: State and parameter identification via joint and dual extended Kalman filters. *Comput. Methods Appl. Mech. Eng.* **2005**, *194*, 5242–5272.

20. Akhlaghi, S.; Zhou, N.; Huang, Z. Adaptive adjustment of noise covariance in Kalman filter for dynamic state estimation. In Proceedings of the 2017 IEEE Power & Energy Society General Meeting, Chicago, IL, USA, 16–20 July 2017; pp. 1–5. https://doi.org/10.1109/PESGM.2017.8273755.
21. Eftekhar Azam, S.; Mariani, S. Online damage detection in structural systems via dynamic inverse analysis: A recursive Bayesian approach. *Eng. Struct.* **2018**, *159*, 28–45. https://doi.org/10.1016/j.engstruct.2017.12.031.
22. Hughes, T.J.R. *The Finite Element Method*; Dover Publication: New York, NY, USA, 2007.